polymer communications

Characterization of fibres from poly-(2-fluorophenylene-2-fluoroterephthalamide) by a combination of WAXD and AFM studies

B. H. Glomm, M. C. Grob, P. Neuenschwander and U. W. Suter*
Institut für Polymere, Eidgenössische Technische Hochschule (Swiss Federal Institute of Technology), CH-8092 Zürich, Switzerland

and D. Snětivy and G. J. Vancso*
Department of Chemistry, University of Toronto, 80 St. George Street, Toronto, Ontario, M5S 1A1, Canada
(Received 3 June 1993; revised 27 September 1993)

Wide-angle X-ray diffraction (WAXD) and atomic force microscopy (AFM) were used to study the crystallographic structure of poly-(2-fluorophenylene-2-fluoroterephthalamide) fibres. The unit cell parameters were obtained in WAXD measurements, and AFM yielded complementary information about the conformation of the fluorine-substituted phenylene rings. Results are compared with predicted crystal structures of poly(*p*-phenyleneterephthalamide) fibres, which were obtained by computer simulation experiments.

(Keywords: crystal structure; WAXD; polyamides)

Introduction

Rigid-rod, *para*-substituted, fully aromatic polyamides display high thermal resistance, tensile strength and modulus when processed into fibres from nematic solutions[1,2]. The introduction of substituents, especially halogens with controlled substitution patterns, into aromatic polyamides is a well-known path for modification of the macroscopic physical and chemical properties of both the polymer solutions and the fibre materials produced from these solutions[3–8].

We have synthesized regular head-to-tail[9] poly(2-fluorophenylene-2-fluoroterephthalamide) (FPFT) [IUPAC name: poly(2-fluoro-phenylene-1,4-diyl-imino-2-fluoroterephthaloyl-imino)] and processed it into fibres. This material has been fully characterized by wide-angle X-ray diffraction (WAXD) and atomic force microscopy (AFM). The synergistic combination of WAXD and AFM yields detailed structural information not available by the individual techniques alone.

WAXD has been the traditional technique of choice for obtaining information on the crystal structure of partially crystalline polymers, including unit cell parameters, chain packing and crystallite sizes. However, lattice distortions in the fibre crystal structure and small crystals broaden the lines in the WAXD pattern, often making detailed structure determination difficult or incomplete. In addition, polymorphism often makes interpretation of WAXD data inconclusive[10]. With the advent of AFM, an experimental tool became available to study the molecular architecture by direct visualization of atoms and molecules at the surface of polymeric materials[11–17]. Molecular imaging and the study of polymorphism in fibres of poly(*p*-phenyleneterephthalamide) (PPTA) have already been reported[18]. This paper demonstrates that AFM often yields complementary information about the nanostructure and conformation of polymers which is not accessible through the use of WAXD.

Experimental

Sample preparation. FPFT powder[9] was dissolved in 100% w/w H_2SO_4, dry-jet wet-spun through a 1 cm air gap into an aqueous coagulation bath and subsequently collected on a wind-up roller with a draw ratio of 0.67 (flow velocity at the spinerette:wind-up velocity). The fibre sample discussed in this work was spun at 25°C, with a velocity of 20 m min^{-1}, from a 15% w/w polymer-in-acid solution into a 2°C bath using a monofilament spinerette with a diameter of 100 μm.

The fibre was washed in water for 24 h and annealed for 12 s at 400°C under an argon atmosphere with a constant tensile stress of 150 MPa. Its diameter was determined by light diffraction[19].

WAXD. Raw data on a fibre bundle of about 200 monofilaments were collected using a Siemens D500 diffractometer equipped with CuKα X-ray source, pinhole collimator, Huber texture goniometer, graphite flat crystal monochromator, and scintillation detector. The measurements were performed in $\theta/2\theta$ transmission mode with 2θ from 5 to 55° (step size 0.25°). Fibre diagram quadrants were measured in the range of azimuthal angle, χ, from 0 to 90°. The measurement times per step were adjusted so that the signal-to-noise ratio was better than 95%. Data were corrected for background scattering and smoothed with a low pass filter. Scanning the scattering angle 2θ at $\chi = 0°$ (i.e. perpendicular to the fibre axis) yields an *equatorial* trace. A measurement as a function of 2θ with $\chi = 90°$ (i.e. parallel to the fibre axis) provides a *meridional* trace.

* To whom correspondence should be addressed

0032-3861/94/04/0878–04

AFM. Single FPFT fibres were embedded in epoxy resin (Araldit® standard, Ciba-Geigy), and cleaved along the fibre direction using a Sorval MT6000 ultramicrotome equipped with glass knives. AFM images were taken in air using a NanoScope II instrument (Digital Instruments, Santa Barbara, CA) with an A-type scan head and NanoProbe 100 μm triangular Si_3N_4 microcantilevers with thick legs. The effective spring constant, as specified by the supplier, was 0.38 N m^{-1}. Imaging was performed in the constant deflection mode (the deflection of the cantilever is held constant by the electronic feedback loop and the vertical displacement of the piezo scanner, which is needed to maintain the chosen deflection, is recorded as the sample is scanned under the tip; for a detailed description see ref. 20). Raw data of images with molecular resolution were obtained with the low pass filter set to 1 and the high pass filter to 4. The images were stable and reproducible. Electrostatic charges sometimes caused problems, especially after sample cleaving; in such cases good quality images were obtained after a 24 h waiting period. Graphite and mica images with angstrom resolution were used for distance calibration of the lateral position of the piezo scanner. Horizontal calibration of the scan-head was performed by taking into account the specimen height with respect to the top end of the piezo tube. This procedure (described in ref. 21) has proved to be essential to eliminate systematic errors.

Results and discussion

Before the thermal post-spin treatment, the dry FPFT fibres had an average diameter of 29 μm, which decreased slightly to 28 μm after annealing. The apparent orientation angle, ξ, of the macromolecules, determined from the full-line width of the most intense equatorial reflection in an azimuthal scan[22,23], was 56° for the as-spun fibres. After the annealing procedure this orientation angle was reduced to 17°, a value typical for a good chain orientation of commercial aramid fibres[2,23–25].

Experiments and calculations on PPTA[8] and PPTA derivatives[26,27] show that the substitution of the PPTA skeleton with small substituents does not cause significant changes to the conformation of the molecular backbone or the parallel chain alignment when compared with a PPTA chain. The indexing of the meridional reflections was based on this analogy. The identity period for a regular head-to-tail ordered structure in the c direction (corresponding to the fibre axis) must be about 13 Å. The indexing of equatorial and pseudo-equatorial reflections, which are sensitive to the symmetry of the packing, is also possible by using structural analogies to PPTA. Refinement of these assignments is possible with a minimizing algorithm[28] that fits an idealized unit cell to the measured WAXD data after a first, rough indexing 'by hand'.

Figure 1 shows a quadrant from the WAXD fibre pattern of the annealed FPFT fibres with equatorial and meridional traces. The most intense equatorial and meridional reflections with the corresponding diffraction intensities and Miller indices are shown in *Table 1*. The intensity values were obtained by numerical fits of the line profile, and normalized to the (2 1 0) peak. For

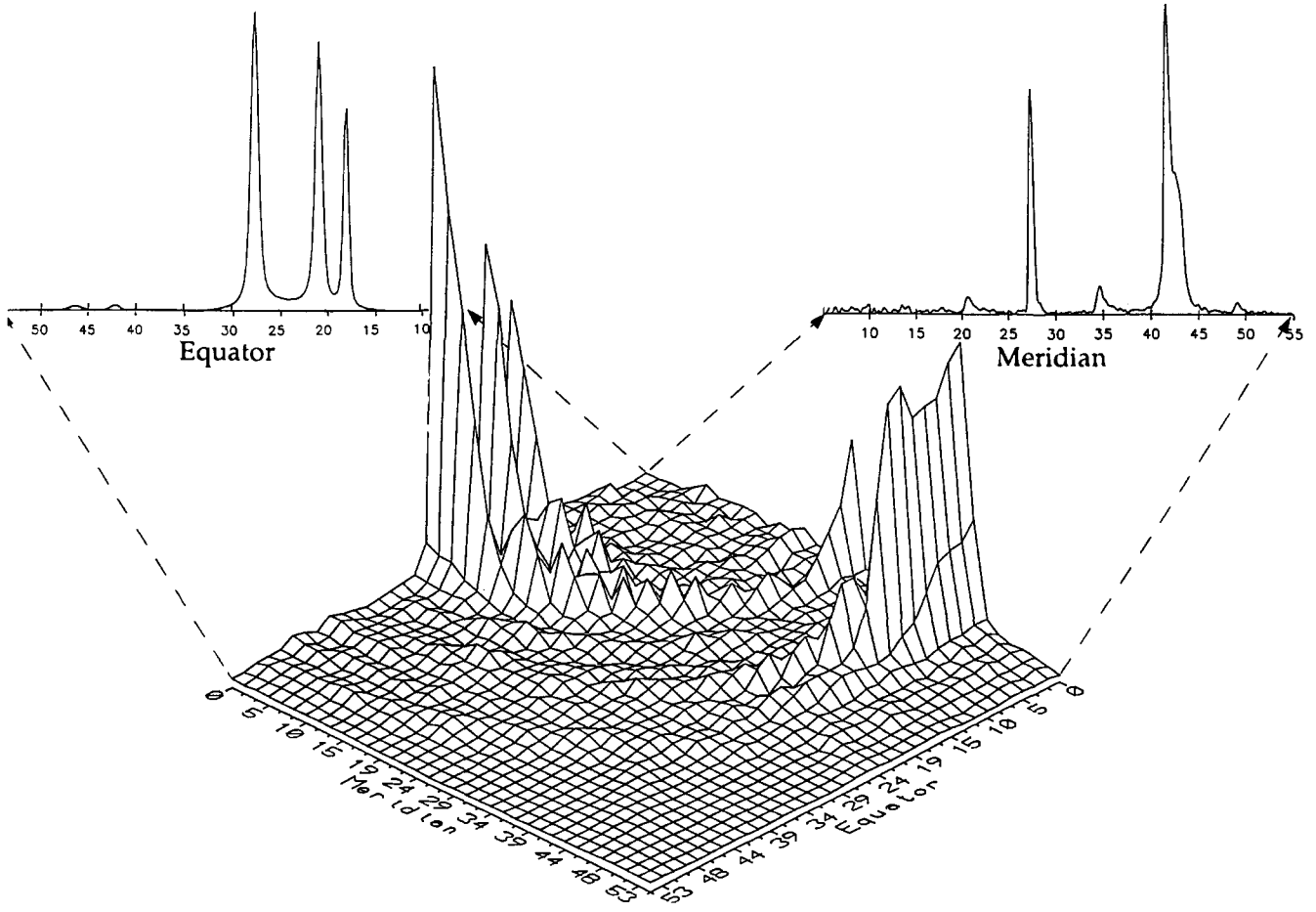

Figure 1 A quadrant of the WAXD pattern for a FPFT fibre spun at a nominal draw ratio of 0.67 after 12 s annealing, including projections from the equatorial (perpendicular to the fibre axis) and meridional (parallel to the fibre axis) intensity traces (2θ scales in degrees)

Table 1 WAXD data obtained on FPFT fibres

2θ (deg)	χ (deg)	d_{hkl} (Å)	I_{rel}[a] (%)	($h k l$)
13.6	90	6.51	vw	(0 0 2)
17.9	0	4.96	42	(0 1 0)
20.6	90	4.31	w	(0 0 3)
20.7	0	4.29	85	(2 0 0)
27.4	90	3.26	18	(0 0 4)
27.7	0	3.22	100	(2 1 0)
34.7	90	2.59	m	(0 0 5)
41.8	90	2.16	24	(0 0 6)
42.1	0	2.15	2	(4 0 0)
46.3	0	1.96	3	(4 1 0)
49.3	90	1.85	w	(0 0 7)

[a] m, medium; w, weak; vw, very weak

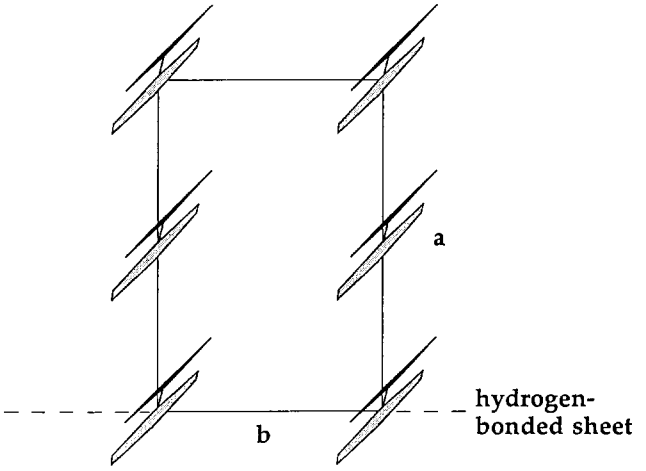

Figure 2 Schematic representation of the *ab* facet of the crystal unit cell of FPFT (projection of the unit cell viewed from the crystallographic *c* direction)

diffraction lines with weak intensities the following notation was used: m, medium; w, weak; vw, very weak. Qualitative transformations in the WAXD pattern, caused by the heat treatment, could not be observed.

As the constitution of the fibres is regularly head-to-tail ordered[9], we indexed the WAXD pattern on the basis of a 'pseudo-orthorhombic' and 'pseudo-edge-centred' cell of head-to-tail chains. This preferred structure is closely related to the 'pseudo-edge-centred' modification II described for the PPTA fibres[29,30], and has the cell edges $a = 8.6$ Å, $b = 5.0$ Å and $c = 13.0$ Å. This structure is also very similar to the PPTA structures 5 and 7 predicted by computer simulation[28]. The two calculated structures differ in the conformation of successive phenylene rings along the chain axis. The phenylene rings of the predicted structure 5 are rotated in the opposite direction with respect to the planar amide group, while the phenylene rings of structure 7 are rotated in the same direction (*Figure 2*). AFM studies of PPTA and the discovery of a new structural polymorphic form[18] have proved that AFM is useful to tackle this problem.

AFM data captured on the surface of a cleaved FPFT fibre are presented in *Figure 3*. Differences in the grey tones correspond to variations in the measured vertical displacement of the piezo-scanner. This AFM nanograph (raw data; scanned area is 5 nm × 5 nm) is typical and exhibits resolution of features on the molecular level. It is worth mentioning that molecular resolution was obtained only in discrete spots on the sample surface over areas of about 25–100 nm^2; this agrees with the average crystallite size measured by WAXD[31]. The fibre sample axis lies at an angle with respect to the scan (horizontal) direction, indicated in *Figure 3* by two markers. The rows on the nanograph pointing in this direction are identified as single macromolecules. Periodicity of the short-range order along the principal directions, i.e. the chain direction and along a line inclined obliquely to that direction, were obtained by analysing the two-dimensional autocorrelation pattern (2-D AP) of the nanograph. The 2-D AP analysis of about 10 images resulted in an average axial periodicity $C/2 = 6.5\ (\pm 0.1)$ Å in the chain direction and a lateral periodicity $B = 5.1\ (\pm 0.1)$ Å with a registration angle $\alpha_{BC} = 85°\ (\pm 1°)$. The axial periodicity is in good agreement with the repeat distance in the crystallographic *c* direction of the crystal structure measured by WAXD. AFM studies of polymorphism in PPTA fibres have shown that the cleavage of the crystals upon microtoming occurs predominantly in the plane of the hydrogen-bonded sheets[18]. This is due to the relatively weak intermolecular forces acting between sheets (compared to the stronger in-plane hydrogen bonding forces). The lateral packing of FPFT chains and the registration angle of the imaged area shown in *Figure 3* are consistent with the parameters of the *bc* facet (the hydrogen-bonded sheet) determined by WAXD. In addition to the information available from WAXD, AFM provides indications of a conformational nature. The pattern generated by the substituted phenylene rings along the axial direction of the FPFT chains clearly indicates a ring inclination in the same direction with respect to the amide group plane (*bc*). This chain conformation is consistent with PPTA structure 7 suggested by computer simulation[28]. The AFM image of this new structure of PPTA[18] has been found to be consistent with successive phenylene rings along the chain being rotated in similar, rather than opposite, directions about the chain axes.

In conclusion, the conventional WAXD technique was

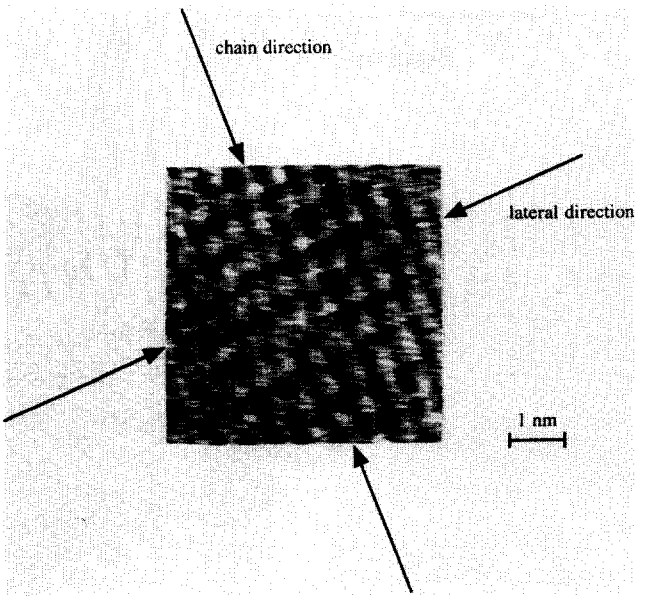

Figure 3 AFM nanograph (image size 5 nm × 5 nm) of a cleaved FPFT fibre. The conjectured chain direction and the lateral direction are shown

used to determine the unit cell parameters of FPFT fibres. AFM yielded complementary information about the conformation of the phenylene rings in FPFT, necessary for the final classification of the structure.

Acknowledgements

Financial support by the Schweizerischer Nationalfonds zur Förderung der wissenschaftlichen Forschung (NF Sektion II), the Stiftung Stipendien-Fonds der Deutschen Chemischen Industrie and the Ontario Center for Materials Research is gratefully acknowledged.

References

1 Morgan, R. J., Pruneda, C. O. and Steele, W. J. *J. Polym. Sci., Polym. Phys. Edn* 1983, **21**, 1757
2 Kwolek, S. L., Memeger, W. and Van Trump, J. E. 'International Symposium on Polymers for Advanced Technology' (Ed. M. Lewin), VCH Publishers, Weinheim, 1987, p. 421
3 Kapuscinska, M. M., Pearce, E. M., Chung, H. F. M., Chang-Chih-Ching and Qu-Xiang-Zhou *ACS Polym. Prepr.* 1983, **24**(2), 337
4 Kapuscinska, M. M. and Pearce, E. M. *J. Polym. Sci., Polym. Chem. Edn* 1984, **2**(12), 3989
5 Nagata, M., Tsutsumi, N. and Kiyotsukuri, T. *J. Polym. Sci. A: Polym. Chem.* 1988, **26**(1), 235
6 Gentile, F. T., Meyer, W. R. and Suter, U. W. *Macromolecules* 1991, **24**, 633
7 Meyer, W. R., Gentile, F. T. and Suter, U. W. *Macromolecules* 1991, **24**, 642
8 Rutledge, G. C., Suter, U. W. and Papaspyrides, C. D. *Macromolecules* 1991, **24**, 1934
9 Grob, M. C., Neuenschwander, P. and Suter, U. W. in preparation
10 Corradini, P. and Guerra, G. *Adv. Polym. Sci.* 1992, **100**, 183
11 Marti, O., Ribi, H. O., Drake, B., Albrecht, T. R., Quate, C. F. and Hansma, P. K. *Science* 1988, **239**, 50
12 Drake, B., Prater, C. B., Weisenhorn, A. L., Gould, S. A. C., Albrect, T. R., Quate, C. F., Cannell, D. S., Hansma, H. G. and Hansma, P. K. *Science* 1989, **243**, 1586
13 Magonov, S. N. and Cantow, H.-J. *J. Appl. Polym. Sci.: Appl. Polym. Symp.* 1992, **51**, 3
14 Snétivy, D. and Vancso, G. J. *Macromolecules* 1992, **25**, 3320
15 Snétivy, D., Guillet, J. E. and Vancso, G. J. *Polymer* 1993, **34**, 429
16 Snétivy, D., Yang, H. and Vancso, G. J. *J. Mater. Chem.* 1992, **2**, 891
17 Snétivy, D., Rutledge, G. C. and Vancso, G. J. *ACS Polym. Prepr.* 1992, **33**, 786
18 Snétivy, D., Vancso, G. J. and Rutledge, G. C. *Macromolecules* 1992, **25**, 7037
19 Perry, A. J., Ineichen, B. and Eliasson, B. *J. Mater. Sci.* 1974, **9**, 1376
20 Sarid, D. 'Scanning Force Microscopy With Applications to Electric, Magnetic, and Atomic Forces', Oxford University Press, Oxford, 1991
21 Snétivy, D. and Vancso, G. J. *Langmuir* 1993, **9**, 2253
22 Rutledge, C. G. and Oertli, A. G. *Makromol. Chem.* 1991, **192**, 2993
23 Blades, H. (E. I. Dupont de Nemours and Co.) US Patent 3 869 430, *Chem. Abstr.* 1975, **78**, 85795w
24 Chatzi, E. G. and Koenig, J. L. *Polym. Plast. Technol. Eng.* 1987, **26** (3&4), 229
25 Ward, I. M. 'Structure and Properties of Oriented Polymers', Applied Science , London, 1975
26 Glomm, B. H., Rutledge, G. C., Küchenmeister, F., Neuenschwander, P. and Suter, U. W. *Makromol. Chem.* submitted
27 Glomm, B. H., Rickert, C., Neuenschwander P. and Suter, U. W. *Makromol. Chem.* submitted
28 Rutledge, G. C. and Suter, U. W. *Macromolecules* 1991, **24**, 1921
29 Haraguchi, K., Kajiyama, T. and Takayanagi, M. *J. Appl. Polym. Sci.* 1979, **23**, 903
30 Haraguchi, K., Kajiyama, T. and Takayanagi, M. *J. Appl. Polym. Sci.* 1979, **23**, 915
31 Hosemann, R. and Bachi, S. N. 'Direct Analysis of Diffraction by Matter', North-Holland, Amsterdam, 1962